Available online at www.sciencedirect.com
ScienceDirect
Biochimica et Biophysica Acta 1770 (2007) 12–23
Biochimica et Biophysica Acta BBA
www.elsevier.com/locate/bbagen

Electroporation in dense cell suspension—Theoretical and experimental analysis of ion diffusion and cell permeabilization

Mojca Pavlin [a,*], Vilko Leben [b], Damijan Miklavčič [a]

[a] University of Ljubljana, Faculty of Electrical Engineering, Tržaška 25, SI-1000 Ljubljana, Slovenia
[b] Iskratel Ltd., Ljubljanska cesta 24a, SI-4000 Kranj, Slovenia

Received 18 January 2006; received in revised form 14 June 2006; accepted 28 June 2006
Available online 11 July 2006

Abstract

Electroporation is a process where increased permeability of cells exposed to an electric field is observed. It is used in many biomedical applications including electrogene transfection and electrochemotherapy. Although the increased permeability of the membrane is believed to be the result of pores due to an induced transmembrane voltage U_m, the exact molecular mechanisms are not fully explained.

In this study we analyze transient conductivity changes during the electric pulses and increased membrane permeability for ions and molecules after the pulses in order to determine which parameters affect stabilization of pores, and to analyze the relation between transient pores and long-lived transport pores. By quantifying ion diffusion, fraction of transport pores f_{per} was obtained. A simple model, which assumes a quadratic dependence of f_{per} on E in the area where $U_m > U_c$ very accurately describes experimental values, suggesting that f_{per} increases with higher electric field due to larger permeabilized area and due to higher energy available for pore formation. The fraction of transport pores increases also with the number of pulses N, which suggest that each pulse contributes to formation of more and/or larger stable transport pores, whereas the number of transient pores does not depend on N.
© 2006 Elsevier B.V. All rights reserved.

Keywords: Electroporation; Ion diffusion; Conductivity; Cell suspension; Electrochemotherapy

1. Introduction

Electroporation is usually described as the formation of transient pores which are formed in the cell membrane in presence of a strong external electric field. The permeable state of the cell membrane lasts up to minutes after the application of electric pulses, which enables transport of molecules and ions that otherwise cannot pass across the cell membrane. Electroporation, known also as electropermeabilization, is used in many important biological and medical applications, the most promising of these being electrochemotherapy of tumors [1–3] and electrogene transfection [4–7]. Yet in spite of successful use of electroporation in biomedical applications the molecular mechanisms of the involved processes are still not fully explained and there is lack of connection between experimental data and theoretical descriptions of pore formation [8–12].

Electroporation has been observed in many different systems, i.e. lipid bilayers, vesicles, cells in vitro and in vivo. The extensive in vitro studies of electroporation [13–16] examining the effect of different parameters (electric field strength, number of pulses, duration) on the extent of permeabilization—uptake of exogenous molecules, cell survival and resealing, have shown that the critical parameter for electroporation is the electric field strength. Permeabilization occurs only above a certain (phenomenological) E_c which is governed by both duration t_E and number of pulses N [10]. It was also shown [14,16] that neither electrical energy, nor charge of the electric pulses alone determine the extent of permeabilization and that the dependency on E, N and t_E is more complex. Post-electroporation membrane resealing lasts for minutes, is strongly temperature dependant and is governed by slow ATP dependant biological processes.

* Corresponding author. Tel.: +386 1 4768 768; fax: +386 1 4264 658.
E-mail address: mojca@svarun.fe.uni-lj.si (M. Pavlin).

0304-4165/$ - see front matter © 2006 Elsevier B.V. All rights reserved.
doi:10.1016/j.bbagen.2006.06.014

Previous more theoretical studies [8–12,17–20] focused on the biophysical aspects of the mechanisms of pore formation. The authors describe formation of hydrophilic pores in the cell membrane, where the change in free energy also depends on the applied electric field strength. For an experimental validation usually measurement of conductivity was made in vitro or with patch-clamp method [17,19,21–26]. The observed transient increase in conductivity during the pulse was explained by the formation of transient pores in the cell membrane. However, this short-lived transient pores cannot explain increased long-lasting permeability of the membrane, which is observed after the pulses.

Based on all these studies it became clear that the relation between transient conductivity changes (transient pores) and transport after the pulses (long-lived pores) is more complex and cannot be explained with theories which only analyze the transient pores during the electric pulses. Only few studies, directly observed and quantified the actual transport across the membrane and analyze the relation between transient changes and long-lived increased permeability of the cell membrane [21–23,26–29]. There is also no general agreement of how the long-lived transport pores become stable and enable transport of molecules as large as DNA.

The main focus of our study is exactly in trying to connect the findings and theoretical description on the level of pore formation and increased membrane conductivity during the electric pulses with direct observation and quantification of increased transport for ions and molecules after the pulses. In order to achieve this, we analyze in parallel the transient pores and the transport pores, how they depend on the electric field and the number of pulses, and the relation between short-lived transient pores and the transport pores. We measured together the observable quantities, which indicate increased membrane permeability: (i) the transient conductivity changes during the pulses (related to transient pores), and (ii) the ion efflux and (iii) the transport of molecules after the pulses (both related to long-lived pores). We performed experiments where the conductivity of a dense cell suspension was measured during and after the application of electrical pulses in a low-conductive medium. We analyzed how electric field strength and the number of pulses affect transient conductivity changes and the ion efflux, and compare both to transport of molecules. We further used diffusion equation to quantify the time dependent ion efflux and present a simple model, which describes the permeability of the membrane (the fraction of long-lived pores) for applied electric field strength and for a given number of pulses.

2. Materials and methods

2.1. Electroporation and current–voltage measurements

The experimental setup consisted of a generator that delivered square pulses, an oscilloscope and a current probe. Two high-voltage generators were used; for protocol where 8×100 μs pulses were used (Fig. 1a) a prototype developed at the University of Ljubljana, Faculty of Electrical Engineering, was used and for the second protocol to deliver N×100 μs+8×1 ms pulses Cliniporator™ (IGEA s.r.l., Carpi, Modena, Italy) device was used, which allowed us to deliver two sets of pulses with a given delay in between (Fig. 1b).

During the pulses the electric current was measured with a current probe (LeCroy AP015, New York, USA) and the applied voltage with the high-voltage probe (Tektronix P5100, Beaverton, USA). Both current and voltage were measured and stored on the oscilloscope (LeCroy 9310 C Dual 400 MHz, New York, USA). In the first experimental protocol we used a train of eight square pulses of 100 μs duration with 1 Hz repetition frequency (8×100 μs protocol). Pulse amplitudes were varied to produce applied electric fields $E_0=U/d$, between 0.4 and 1.8 kV/cm. In the second experimental protocol first a given number N (1, 2, 4 and 8) of 100 μs pulses with repetition frequency 10 Hz were delivered, and after a delay of 4200 ms after the first pulse eight 1 ms test pulses of the same amplitude with the repetition frequency 1 Hz were delivered (N×100 μs+8×1 ms pulsing protocol). The frequency should not effect permeabilization neither the diffusion of ions, since it was shown that the relaxation of conductivity after the pulse is few ms [26] and that changing the pulse repetition frequency between 1 Hz and 1 kHz does not influence significantly the transport of small molecules [30]. The 8×1 ms test pulses were used to determine post-pulses conductivity changes after 4200 ms and the maximum increase (1 ms long pulses were used due to the limitation of the pulse generator, but since only the initial level of the conductivity of the first pulse was analyzed and other pulses were used to determine the maximum conductivity increase, this had no effect on the results).

Each type of experiments was repeated twice. The amplitudes of N pulses in the train and the test pulses were set to voltage which gave applied electric field E_0=1 kV/cm. The memory segmentation function of the oscilloscope was used in order to obtain high time resolution during the pulses and only 100 μs after the pulses were recorded. Parallel aluminum plate electrodes (Eppendorf cuvettes) with 2 mm distances between the electrodes were used. For every set of parameters a reference measurement on medium with no cells was also performed.

2.2. Cells and medium

Mouse melanoma cell line, B16F1, was used in experiments. Cells were grown in Eagle's minimum essential medium supplemented with 10% fetal bovine serum (Sigma-Aldrich Chemie GmbH, Deisenhofen, Germany) at 37 °C in a humidified 5% CO_2 atmosphere in the incubator (WTB Binder, Labortechnik GmbH, Germany). For all experiments the cell suspension was prepared from confluent cultures with 0.05% trypsin solution containing 0.02% EDTA (Sigma-Aldrich Chemie GmbH, Deisenhofen, Germany). From the

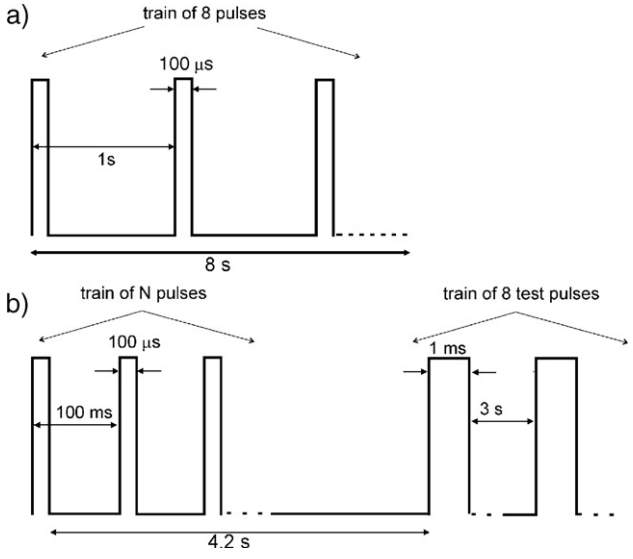

Fig. 1. The two pulsing protocols. In one set of experiments a train of eight pulses 8×100 μs with repetition frequency 1 Hz was delivered (a). In the second set of experiments we used a sequence of N=1, 2, 4 and 8 pulses with repetition frequency 10 Hz and after a delay (between the first pulse and first test pulse), which was set to be 4200 ms, a train of eight test pulses of the same amplitude as of the first pulses was delivered—a N×100 μs+8×1 ms protocol (b).

obtained cell suspension trypsin and growth medium were removed by centrifugation at 1000 rpm at 4 °C (Sigma, Germany) and the resulting pellet was resuspended in medium and again centrifuged. A low-conductive medium was used for electroporation that contained phosphate buffer with 250 mM sucrose—PB σ_0 (25 °C)=0.127 S/m. In all the experiments dense cell suspensions having cell volume fractions F=0.3 (1×10^8 cells/ml) were used.

3. Theory

In this section we discuss theoretical background of electroporation: (i) first the induced transmembrane voltage, which is crucial for electroporation, than (ii) the transport through the permeabilized cell membrane after the electric pulses and finally (iii) increased conductivity of permeabilized cells due to the formation of transient pores during the electric pulses.

3.1. The induced transmembrane potential

When a cell is exposed to an external electric field E the induced transmembrane voltage U_m is generated on the cell membrane due to the difference between the electric properties of cell membrane, the cytoplasm, and external medium, known as the Maxwell–Wagner polarization. The induced transmembrane voltage on a non-permeabilized spherical cell for a step turn-on of DC electrical field can be derived from the Laplace equation, which gives a time dependent solution for the induced transmembrane voltage on a cell membrane [9]. After a charging time ($t>10^{-7}$ to 10^{-6} s) the transmembrane voltage can be approximated (except in very low-conductive medium) with

$$U_m = 1.5\ ER\cos\theta, \tag{1}$$

where it is assumed that the cell membrane is almost non-conductive compared to the external medium, R is the cell radius and θ is the angle between direction of the electric field and the point vector on the membrane. For cells in suspension or in tissue we have to take into account also a decrease in the local electric E due to surrounding cells, which reduces the induce transmembrane voltage [31].

When the induced transmembrane voltage exceeds the threshold voltage U_c [between 0.2 and 1 V] the part of the cell membrane where $|U_m|>U_c$ is permeabilized [28]—the structural changes in the membrane (pores) are formed. The permeabilized part of the cell membrane can be therefore defined by the critical angle θ_c, where $U_c=1.5\ ER\cos\theta_c$. Now, we define the critical field as the electric field where $\theta_c=0$: $E_c=U_c/1.5\ R$ and thus obtain the formula for the surface area of two spherical caps exposed to above-threshold transmembrane voltage (brighter shaded region in Fig. 2):

$$S_c = S_0(1 - E_c/E), \tag{2}$$

where S_0 is the total surface area of the cell. From Eq. (2) and Fig. 2 it is evident that the local electric field E is the critical parameter for permeabilization since it defines the area of the membrane which is permeabilized—$S_c(E)$ and through which ionic and molecular transport occurs.

The increased conductivity of the membrane in the permeabilized region decreases the induced transmembrane voltage U_m for $\theta<\theta_c$ [32–36] leading to a more complex, time-dependent U_m, which is governed by the electric field strength, electrical properties of cell and medium, and pulse duration [29,32].

3.2. Transport through the permeabilized membrane

In general the increase in membrane permeability for ions and molecules can be described as the fraction of the permeable surface of the cell membrane which can be also defined as the fraction of all "transport" pores:

$$f_{per} = S/S_{tot} = S_{por}/S_0. \tag{3}$$

where S_{por} represents the area of pores of one cell, S total area of all pores, S_0 area of one cell and S_{tot} total area of N cells. The parameter f_{per} represents the fraction of the long-lived pores which are large enough to contribute to increased permeability, where the term permeability defines increased diffusion for ions and molecules through the cell membrane. Different studies showed that diffusion of ions and molecules occurs only through the permeabilized area S_c given with Eq. (2), i.e. area which is exposed to above-critical voltage as described in previous section [35,36]. We can therefore derive a diffusion equation, which describes the flux of a given molecule due to the concentration gradient through the permeabilized part of the membrane:

$$\frac{dn_e(t)}{dt} = -\frac{c_e(t) - c_i(t)}{d} D f_{pc}(E, t_E, N)\ (1 - E_c/E) S_0, \tag{4}$$

where $f_{per}=f_{pc}(1-E_c/E)$, and f_{pc} $(E,\ t_E,\ N)=S_{por}/S_c$ represents the fraction of pores in the permeabilized region, n_e is the

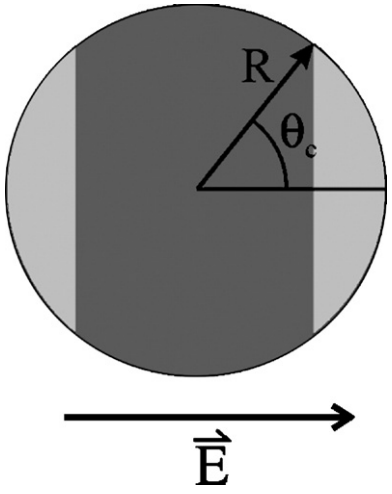

Fig. 2. A spherical cell exposed to the external electric field. The bright shaded part represents the area exposed to above-threshold transmembrane voltage $|U_m|>U_c$, i.e., the permeabilized region, which can be calculated from Eq. (2): $S_c=S_0(1-E_c/E)$.

number of moles in the external medium, D is the diffusion constant and c_e and c_i are the molar concentrations outside and inside of the cell. The above equation describes also the diffusion of ions through the permeabilized region since diffusion is a relatively slow process, which occurs mainly after the pulse application and thus the Nernst–Planck equation simplifies to the above equation, for derivation see Appendix. Even though some form of this equation was written to describe transport through permeabilized membrane, the dependence of f_{pc} on parameters E, t_E, and N was not given explicitly or determined from the measurements.

3.3. Conductivity of permeabilized cells

A transient increase in in vitro conductivity of cells can be explained by the formation of transient pores. The permeabilized part of the cell membrane has increased conductivity σ_m, where σ_m in general depends on the fraction of pores and conductivity of a single pore [36,28]. An increase in single cell conductivity depends on the region of the permeabilized surface S_c where $|U_m| > U_c$ and in general depends on the number and size of the pores, which are formed in the permeabilized part of the cell membrane.

For a cell suspension the bulk (effective) conductivity can be obtained from the conductivity of a single cell σ_p for given volume fraction of cells, which we described earlier [37]. Briefly, a cell suspension is a heterogeneous mixture of cells and surrounding medium and therefore some effective medium theory equation can be used. Effective medium theories (EMT) are only approximate therefore an adequate equation has to be used for a given problem [37–41]. To obtain the change in permeabilized membrane conductivity from measured conductivity of a cell suspension σ we used Maxwell EMT equation [41]

$$\frac{\sigma_e - \sigma}{2\sigma_e + \sigma} = F\frac{\sigma_e - \sigma_p}{2\sigma_e + \sigma_p}, \tag{5}$$

where σ is the effective (measured) conductivity of a suspension of permeabilized cells, σ_p the conductivity of a single cell, F is the volume fraction of the cells and σ_e the conductivity of the external medium. The transient change of the conductivity $\Delta\sigma_{tran} = (\sigma - \sigma_0)$ depends on the average membrane conductivity of the permeabilized area σ_m and on critical angle of permeabilized area θ_c. If $\Delta\sigma_{tran}$ is measured the fraction of transient pores during the pulse (f_p) can be obtained from the transient conductivity changes, where $\Delta\sigma_{tran}$ is a rather complex function of F, E and other parameters. In our previous studies [26,36] we presented a theoretical model, which enables calculation of σ_m and f_p from $\Delta\sigma_{tran}$ and vice versa for different parameters (F, E, σ_e…). We obtained the equation for fraction of transient pores: $f_p = (1 - E_c/E)\sigma_m/\rho(E)\sigma_{por0}$ (for derivation and definition of symbols see reference [26]). Here we have to stress that we have to distinguish between the fraction of transient pores during the pulse (f_p) from the fraction of long-lived "transport" pores after the pulses (f_{per}) as defined in previous section. These are two different physical parameters which have to be analyzed separately.

4. Results

In our present study we performed experiments where the conductivity of a cell suspension was measured during and after the application of pulses. We used a dense cell suspension having a cell volume fraction, $F = 0.3$, and pulse parameters typically used for cell electroporation. A low-conductive medium (Joule heating can be neglected) without K^+ ions was used to obtain efflux of K^+ ions from cells between and after pulses. Two different sets of measurements using two pulsing protocols (see Fig. 1) were made in order to analyze the relation between the transient conductivity changes during the electric pulses (transient increase in permeability) and long-lived permeability of cell membrane by measuring the increase in conductivity of a cell suspension due to the ion efflux. We compared both transient changes and after pulse changes with the uptake of molecules for one and several pulses.

From measured voltage and current signals we obtained the time dependent conductivity of each sample $\sigma(t) = I(t)/U(t)\ d/S$, where d is the distance between the electrodes, and S is the surface of the sample volume at the electrodes. In the first set of experiments (Fig. 1a) we obtained conductivity of the cell suspension σ during a train of eight 100 μs pulses and applied electric field between 0.4 kV/cm and 1.8 kV/cm, as shown in Fig. 3. The fraction of the transient short-lived pores was determined based on measured transient conductivity changes during the electric pulses ($\Delta\sigma_{tran} \Rightarrow f_p$), whereas the fraction of long-lived transport pores (related to the increased membrane permeability after the pulses) was determined from the increase in conductivity between the pulses due to the ion efflux ($\Delta\sigma \Rightarrow f_{per}$).

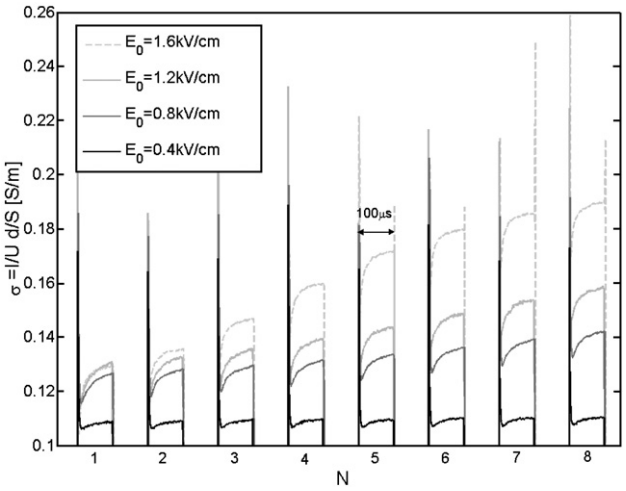

Fig. 3. Measured time dependent conductivity $\sigma(t) = I(t)/U(t)\ d/S$ using a train of eight 100-μs pulses, 1 Hz repetition frequency for different applied electric fields $E_0 = U/d$. The memory segmentation function of the oscilloscope was used in order to obtain high time resolution during the pulses, and only 100 μs after the pulse were recorded.

4.1. Transient conductivity changes

In order to establish the relationship between transient conductivity changes and post-pulse conductivity changes due to ion diffusion, only the difference in the initial and final level of the conductivity was analyzed and not its dynamic behavior. The initial value of conductivity at the start of each pulse σ_0^N was determined three microseconds after the start of the individual pulse, so that fast transient effects due to displacement current and electrode effects were not taken into account. The conductivity at the end of each pulse σ^N was determined and from this the change in the conductivity during the N-th pulse was obtained: $\Delta\sigma_{\text{tran}}^N=\sigma^N-\sigma_0^N$. With σ_0 we denote the initial conductivity at the start of the first pulse $\sigma_0=\sigma_0^1$. Results are presented in terms of the local electric field E rather than applied electric field $E_0=U/d$ since for a high density of cells that we use the local field experienced by each cell is smaller than the applied field due to the interaction between the cells [31]. The ratio E/E_0 was taken from our previous study [31], where the reduction of the local field E (and hence induced transmembrane voltage) due to the neighboring cells was calculated to be 9% for volume fraction of cells $F=0.3$.

In Fig. 4 we show transient conductivity changes $\Delta\sigma_{\text{tran}}^N/\sigma_0$ during the N-th 100 μs pulse for $E_0=U/d=[0.4–1.8]$ kV/cm.

An increase in transient conductivity changes during the pulses $\Delta\sigma_{\text{tran}}^N/\sigma_0$ is observed for E above 0.5 kV/cm. The reference measurements in pure PB medium show slowly increasing $\Delta\sigma^1/\sigma_0$ which can be attributed to electrode processes. Conductivity changes $\Delta\sigma_{\text{tran}}^N/\sigma_0$ for $N>1$ increase up to 1.2 kV/cm and reach maximum (during the first pulse the changes increase up to 1.6 kV/cm). The large increase of the transient conductivity above 0.5 kV/cm agrees with the permeabilization threshold that was determined for this cell line (B16F1) in our previous studies [26] where observable uptake of molecules was obtained above 0.5 kV/cm. If we use this value for E_c we obtain the critical transmembrane voltage for B16F1 cell line, $U_c=670$ mV. From Fig. 4 it can be seen that transient conductivity changes are very similar for the first and

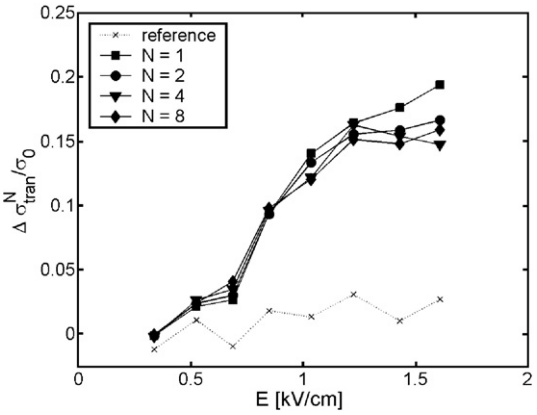

Fig. 4. Transient conductivity changes during N-th pulse. The results are shown for the train of 8×100 μs pulses, $\Delta\sigma_{\text{tran}}^N$ is normalized to the initial conductivity. Solid line—cells in low conductive medium, dotted line—reference measurement on medium without cells during the first pulse. The results are shown against the local electric field E, where $E/E_0=0.91$.

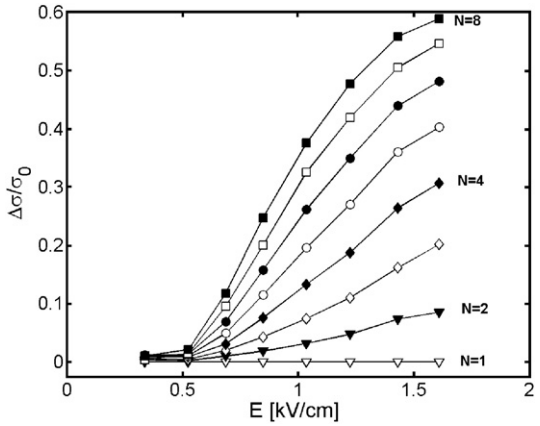

Fig. 5. Relative changes of conductivity between the pulses (the changes of the initial level) in PB medium for eight consecutive pulses: $\Delta\sigma/\sigma_0=(\sigma_0^N-\sigma_0)/\sigma_0$, where σ_0^N is the initial level at the start of the N-th pulse. 8×100 μs pulses were used with repetition frequency 1 Hz (pause between the pulses was 1 s).

all consecutive pulses. This is due to fast relaxation of the conductivity in few ms after the pulses, where conductivity returns almost to the initial level as shown previously [21–26] and thus represent short-lived transient structures—pores. From measured $\Delta\sigma_{\text{tran}}^N/\sigma_0$ we obtained that fraction of transient pores at $E=0.86$ kV/cm is $f_p\approx 3\times10^{-5}$.

4.2. Post-pulse conductivity changes, ion diffusion and membrane permeability

Since we are interested in the long-lived permeability of the membrane and the nature of long-lived pores we have to observe either the transport of ions (K^+, Ca^{++}, ...) or the transport of molecules (PI, bleomycine, lucifer yellow, ...). For this reason we analyzed the increase of the conductivity between the pulses (changes of the initial level) for the consecutive pulses (see Fig. 3). These, relatively slow changes in conductivity can be attributed to the ion efflux which occurs between and after the pulse(s), the ion efflux during the pulses can be neglected due to short duration pf pulses. In Fig. 5 relative changes of the initial level of conductivity at the start of the N-th pulse $\Delta\sigma/\sigma_0=(\sigma_0^N-\sigma_0)/\sigma_0$ for consecutive pulses are shown for increasing electric field. The results are corrected for the effect of colloid osmotic swelling according to our previous study [26], where we have shown that in few seconds after pulse application swelling of cells reduces the measured conductivity of cell suspension in PB medium. Here we have to stress, that in some different pulsing medium, which contains a large amount of large molecules and only small amount of ions outside the cell compared to concentrations in the cytoplasm, the effect is reversed and the cells shrink [27].

In Fig. 5 similarly as in Fig. 4 the initial level starts to increase for $E>0.5$ kV/cm, which can be explained with the efflux of ions mainly K^+ ions from the cytoplasm into the medium through membrane pores due to the concentration gradient (external concentration of K^+ ions is negligible). Consistently with the transient changes also the ion efflux indicates that the cell membrane is permeabilized above

E=0.5 kV/cm. For higher electric fields the efflux of ions increases for higher electric field strengths up to 1.6 kV.

It is clear (Fig. 5) that both, the electric field and the number of pulses, influence the efflux of ions. Therefore we made additional set of experiments with using second pulsing protocol (N×100 μs + 8×1 ms), where first a sequence of N (1, 2, 4 and 8) pulses with 10 Hz were delivered. Then after 4.2 s a train of test pulses of the same amplitude was delivered in order to determine the differences in the fraction of permeabilized surface and the efflux coefficient for different number of pulses. In Fig. 6 the results of the conductivity changes between the pulses are shown using N×100 μs+8×1 ms pulses of E=0.86 kV/cm where 1 (a), 2 (b), 4 (c) and 8 (d) pulses were delivered first (squares), and after 4.2 s between the first pulse and the first test pulse a train of eight test pulses was delivered (circles).

It can be seen that the number of pulses affects the relative change of the conductivity and that after several test pulses also the maximum change is reached, which was used as normalization constant $\Delta\sigma_{\max}$ for each experiment (a, b, c, d). As we show in the Appendix, the changes in the conductivity due to the ion efflux between the consecutive pulses can be described adequately with the diffusion equation, which gives:

$$\frac{\Delta\sigma^N(t)}{\Delta\sigma_{\max}} = \left[1 - \exp\left(-\frac{t}{\tau_N}\right)\right] \quad \tau_N = \frac{dR(1-F)}{f_{per}3D'}, \tag{6}$$

where τ is the diffusion time constant, which depends on the fraction of "transport" pores f_{per}, effective diffusion constants D' (see appendix), cell volume fraction F, thickness of the membrane d and radius of the cell R. It is useful to define efflux coefficient k which is directly proportional to the fraction of the "transport" pores f_{per} and defines the permeable state of the cell membrane

$$k_N = 1/\tau_N = f_{per}\frac{3D'}{dR(1-F)}, \tag{7}$$

where index N denotes that the efflux coefficient and fraction of "transport" pores depends on the number of pulses. In general, also the effective diffusion constant D' can be dependent on N due to different ions mobility for different pore radius, however here we will assume D' as being constant.

From the relative changes in conductivity $\Delta\sigma/\Delta\sigma_{\max}$ presented in Fig. 7 we calculated the efflux coefficient using Eq. (A.8), $k_N = -1/\Delta t_N \ \ln((1-\Delta\sigma_N/\Delta\sigma_{\max})/(1-\Delta\sigma_{\mathrm{test}}/\Delta\sigma_{\max}))$, where Δt_N=[4.2, 4.1, 3.9, 3.5]s is the time delay between last pulse in the train of N pulses and the first test pulse. The efflux coefficient increases with the number of pulses as shown in Fig. 7a (circles).

In order to obtain how efflux coefficients k_N (E) depend on the electric field, we further analyzed the first set of measurements where the whole range of electric fields were used with 8×100 μs pulses. If we plot the time course of the relative changes (the initial levels of the pulses), as shown in Fig. 8a, we can see the time-dependence of the relative conductivity changes due to ion efflux for different number of pulses and different pulse amplitudes. In Appendix we present a simple time-dependent model of the diffusion of the ions which

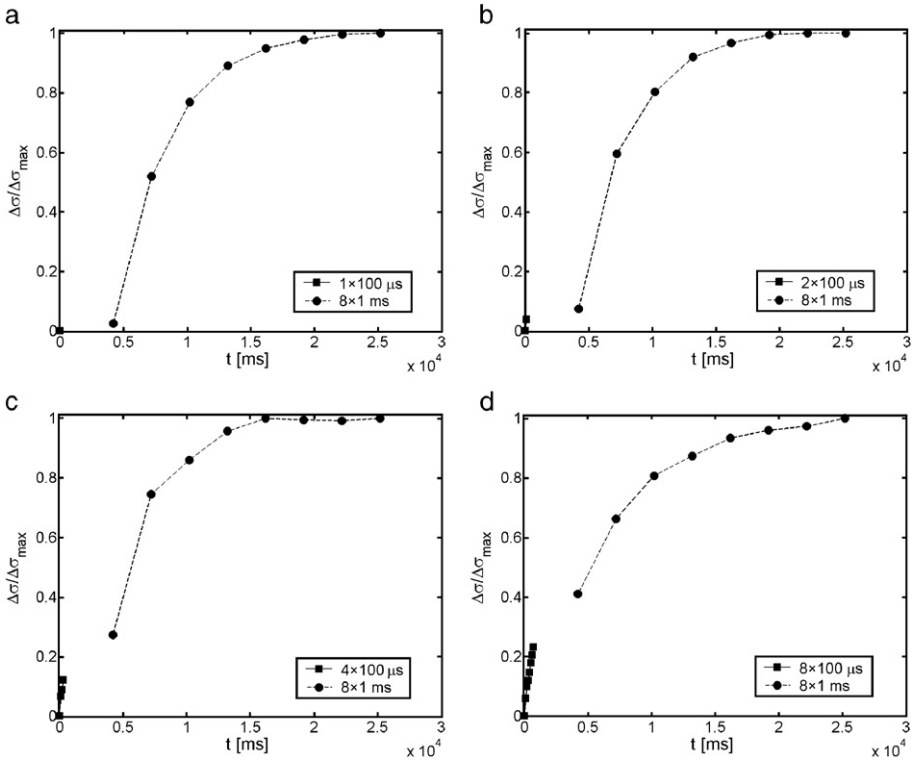

Fig. 6. Measured conductivity changes $\Delta\sigma/\sigma_{\max}$ due to ion efflux using N×100 μs+8×1 ms pulses. Here a sequence of N=1, 2, 4 and 8 pulses with 10 Hz where given. Then after 4.2 s a train of test pulses of the same amplitude was delivered, E=0.86 kV/cm (E_0=1 kV/cm).

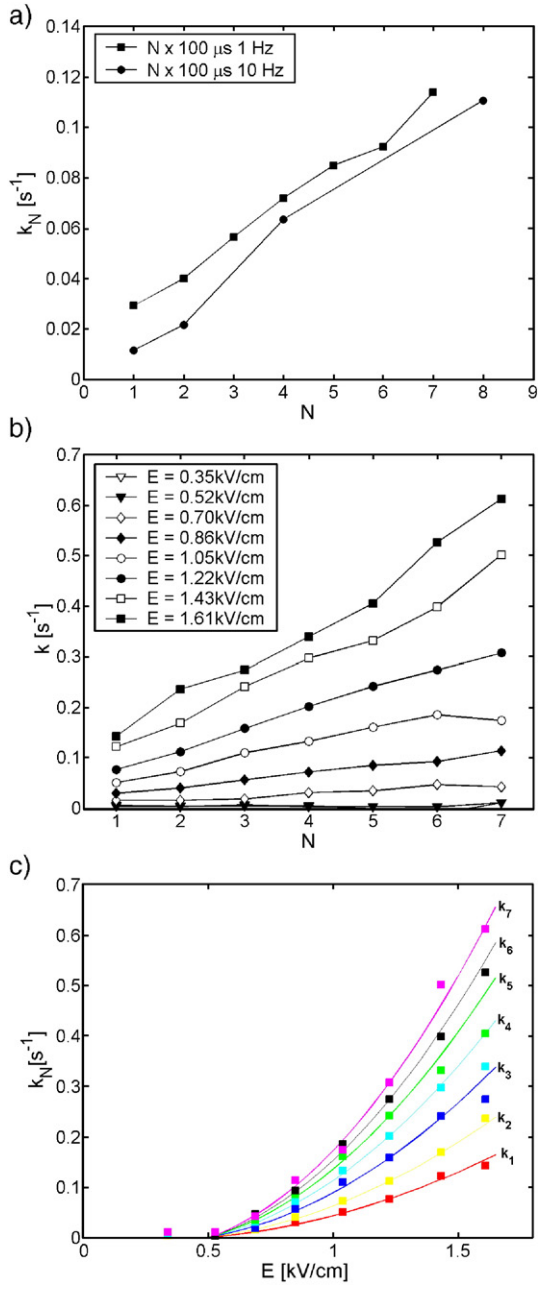

Fig. 7. The efflux coefficients k_N for (a) 1, 2, 4 and 8 pulses obtained from two different protocols calculated from conductivity changes between the pulses $\Delta\sigma/\sigma_{max}$ (see Fig. 6) at $E=0.86$ kV/cm; (b) k_N after the N-th pulse calculated using Eq. (A.8) from the conductivity changes $\Delta\sigma/\sigma_0$ using 8×100 μs pulses and (c) comparison of the prediction of the model according to Eq. (9) (lines) and the measured efflux coefficients (symbols).

incorporates also the efflux coefficient being dependent on the number of pulses, as well as the changes of the volume fraction of cells due to osmotic swelling. If we consider the conductivity changes between the pulses and assume diffusion of ions through the membrane we obtain the efflux coefficient k_N which depends on the number of delivered pulses (see Appendix):

$$k_N = \frac{1}{\Delta t}\ln\left[\left(1-\frac{\Delta\sigma_N}{\Delta\sigma_{max}}\right)\Big/\left(1-\frac{\Delta\sigma_{N+1}}{\Delta\sigma_{max}}\right)\right]. \quad (8)$$

Using the above equation the efflux coefficient can be calculated for different field strengths and number of pulses k_N (E). In Fig. 7a we compare efflux coefficients k_N ($E=0.86$ kV/cm) for both protocols and we can see that good agreement is obtained. In Fig. 7b and c we show k_N for 8×100 μs protocol and it can be observed that k_N's and with this also the fraction of the "transport" pores approximately linearly increase with the number of pulses, and as expected increase also for larger electric field strengths. This analysis shows that the number and/or radius of long-lived "transport" pores increases with number of pulses and E. From k_N at $E=0.86$ kV/cm we obtained the fraction of transport pores ranging from $f_{per}=1.2\times10^{-6}$ at $N=1$ to $f_{per}=4.6\times10^{-6}$ after seven pulses. The fraction of the long-lived transport pores at $E=0.86$ kV/cm is approximately 10-times lower as the fraction of transient pores ($f_{per}=3\times10^{-5}$).

4.3. Comparison of the experimental results and the theoretical model

As already mentioned, in general we can describe the permeable state of the cell membrane with the efflux coefficient k_N which depends on the electric field strength and is proportional to the fraction of the "transport" pores. In the

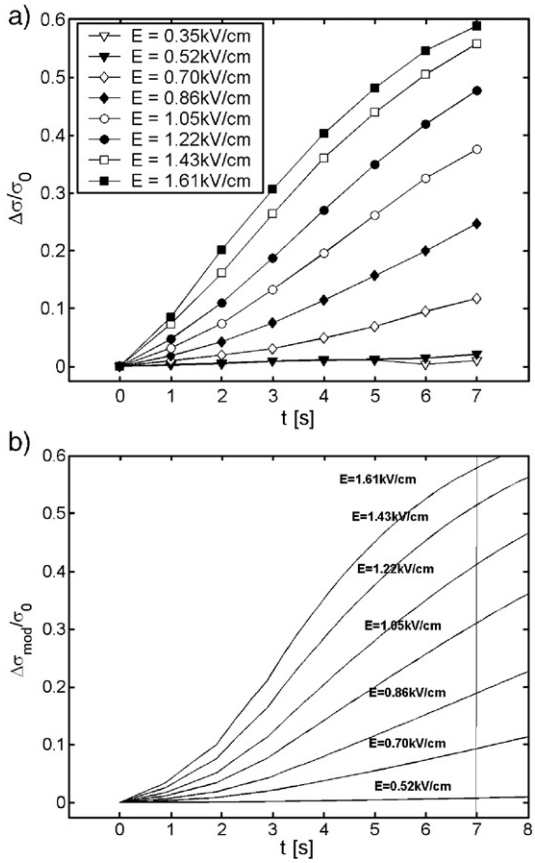

Fig. 8. Time dependent conductivity changes due to ion efflux. (a) Measured conductivity changes (corrected for the effect of colloid osmotic swelling) $\Delta\sigma/\sigma_0$ for 8×100 μs compared to the calculated changes $\Delta\sigma_{mod}/\sigma_0$ due to ion efflux using the theoretical model using Eqs. (9) and (A.8), the k_N's were used from measured values with $N\times100$ μs$+8\times1$ ms protocol (see Fig. 6a).

Theory section we have obtained the equation, which determines how the electric field governs the area of the cell membrane which is exposed to the above-critical transmembrane voltage U_c and has increased permeability: $S_c(E)=S_0(1-E_c/E)$. Furthermore, we can assume that pore formation in the area where $U>U_c$ is governed by the free energy of the pore, where the electrostatic term includes also the square of the electric field $\Delta W_e=aE^2$ [12,18,19]. Based on this we can assume that the most simplified equation, which describes the field dependent permeability, can be written as:

$$k_N(E) = C_N(1 - E_c/E)E^2, \quad (9)$$

where C_N are constants that depend on the size of the "transport" pores and their growth, and are thus dependent also on the number of pulses. The above equation takes into account the increase of the area of the cell exposed to the above critical voltage and the quadratic field dependence in the permeabilized region.

In Fig. 7c we compare the field dependence of the experimental efflux coefficient with the theoretical model. We show the prediction of the theoretical model and the measured efflux coefficient calculated using Eq. (8) from the conductivity measurements for 8×100 μs pulses. Here the constants C_N were determined from the k_N's at $E=1.22$ kV/cm. As expected, the efflux coefficient k_N and with this fraction of "transport" pores (see Eq. (7)) increases above the threshold electric field. More interestingly, this simple model (Eq. (9)) can very accurately describe the measured values, as can be seen in Fig. 7c where lines, which were calculated using the theoretical model (Eq. (9)), coincide with the measured values (symbols). This demonstrates that the formation of long-lived pores is governed also by the energy of the pores, as suggested in other studies [12,17–19,29].

In Fig. 8 we further compare the measured time dependent conductivity changes (mostly due to ion efflux) $\Delta\sigma/\sigma_0$ obtained from the first set of experiments using 8×100 μs protocol (a) and results of the theoretical model (b) where the efflux coefficients were calculated using Eq. (9) for different E from the second set of experiments ($N\times100$ μs$+8\times1$ ms protocol) at $E=0.86$ kV/cm. The integration of the Eq. (A.7) from Appendix yields the time dependent conductivity changes $\Delta\sigma_{mod}/\sigma_0$ as shown in Fig. 8b. The time course as well as the electric field dependence of the model approximately follows the experimental data, except for the slower increase at the start, which can be explained with lower values of the efflux coefficients obtained from the first set of experiments (see Fig. 7a).

Based on these results we can state that a simple model based on a diffusion equation which includes the quadratic field dependence in the region where $U_m>U_c$ can predict the time-dependent ion efflux and change in the post-pulse conductivity as shown in Fig. 8. Comparing the prediction of the theoretical model with the measured efflux coefficients we showed that the fraction of long-lived transport pores increases with higher electric field due to larger area of the cell membrane exposed to above critical voltage as well as due to higher energy which is available for pore formation. In contrast to short-lived pores, where f_p remain the same during each pulse, the fraction of long-lived "transport" pores f_{per} and efflux coefficient k_N increase with each consecutive pulse.

5. Discussion

It was shown that electroporation causes short-lived structural changes in the cell membrane with fast resealing which can be measured by current and voltage measurements during and shortly after the pulses. But more importantly for applications, electroporation causes also long-lasting increased permeable state of the cell membrane, which persists for several seconds and minutes after the pulses and enables uptake of external molecules into the cell and diffusion of ions across the cell membrane.

For successful application of electroporation it is important to understand how the transport through the permeabilized cell membrane is governed by the electric field and the number of pulses, as well as to explain the relationship between the short-lived transient structures (pores) and the long-lived increased permeability of the cell membrane (long-lived pores). This is the focus of the present study, where we investigate together transient conductivity changes, the diffusion of ions and transport of molecules in order to connect on one hand, more theoretical descriptions of electroporation and on the other hand, the experimental measurements of molecule diffusion in vitro. We quantify i) the transient conductivity changes from which fraction of transient (short-lived) pores f_p can be determined; ii) ion diffusion after the pulses from which efflux coefficients k and fraction of long-lived "transport" f_{per} pores can be obtained and iii) compare both (i and ii) with the fraction of permeabilized cells determined with the transport of molecules.

We designed experiments where the conductivity of a cell suspension was measured during and after application of electrical pulses in a low-conductive medium with two sets of pulsing protocols (8×100 μs and $N\times100$ μs$+8\times1$ ms). We obtained, that the measured changes in conductivity of a cell suspension above the critical electric field E_c consists of a transient increase in conductivity during each pulse $\Delta\sigma^N_{tran}/\sigma_0$ with fast relaxation in milliseconds, and conductivity increase in seconds after pulse application due to the efflux of ions from the cell interior—$\Delta\sigma/\sigma_0$. The conductivity changes after the pulses were corrected due to decrease in conductivity caused by colloid-osmotic swelling, [24–26]. The transient conductivity changes as well as conductivity increase due to ion efflux are both observed above the critical electric field (E_c) for permeabilization indicating increased permeability of the cell membrane. Thus for given pulsing protocol conductivity measurements could be used to detect cell permeabilization and to on-line control the voltage and consequently the tissue permeabilization [26,42,43].

In Table 1 comparison between the measured transient conductivity changes $\Delta\sigma^N_{tran}/\sigma_0$ during N-th pulse, changes of the initial level due to ion diffusion $\Delta\sigma/\sigma_{max}$ (N) after N pulses, the fraction of transient pores f_p, the fraction of transport pores

Table 1
Comparison of the measured transient conductivity changes $\Delta\sigma^N_{tran}/\sigma_0$ during N-th pulse, changes of the initial level of conductivity due to ion efflux $\Delta\sigma^N/\sigma_0$ (after N pulses), the fraction of transient pores f_p, the fraction of transport pores f_{per} and the efflux coefficient k_N, to percentage of permeabilized cells at $E \sim 1$ kV/cm

Number of pulses	$N=1$	$N=2$	$N=4$	$N=8$
$\Delta\sigma^N_{tran}/\sigma_0$ transient changes	0.15	0.14	0.14	0.145
$\Delta\sigma/\sigma_{max}$ ion efflux [a]	0.047	0.125	0.27	0.41
f_p transient pores	$\sim 3\times10^{-5}$	$\sim 3\times10^{-5}$	$\sim 3\times10^{-5}$	$\sim 3\times10^{-5}$
f_{per} transport pores	$\sim 1.2\times10^{-6}$	$\sim 1.6\times10^{-6}$	$\sim 2.9\times10^{-6}$	$\sim 4.6\times10^{-6}$
k_N [s^{-1}] $N\times100$ μs $+8\times1$ ms [b]	0.011	0.022	0.063	0.110
k_N [s^{-1}] 8×100 μs [b]	0.029	0.040	0.072	0.114
% permeabilization [c]	10%	–	–	90%
% permeabilization [d]	14%	–	33%	75%

[a] Obtained from Fig. 6, protocol N×100 μs+8×1 ms.
[b] The pulsing protocol which was used.
[c] According to Ref. [16].
[d] According to Ref. [17].

f_{per} and efflux coefficients k_N to percentage of permeabilized cells at $E=0.86$ kV/cm is given (% permeabilization at 1 kV/cm) is presented.

It can be observed that $\Delta\sigma^N_{tran}/\sigma_0$ and the fraction of transient pores f_p are almost identical during the first and each consecutive pulse, whereas permeabilization (transport of molecules) increases with the number of pulses. The transient conductivity changes thus indicate only short-lived pores in the cell membrane that do not contribute to the transport of molecules. On the other hand, the ion efflux $\Delta\sigma/\sigma_{max}$, the efflux coefficients k_N, and fraction of transport pores f_{per} similarly as the transport of molecules increase with number of pulses N. We can therefore use analysis of ion diffusion after the pulses as a method to quantify the fraction of the "transport" pores and long-lasting permeability of the cell membrane. The results in Table 1 clearly show that the transient conductivity changes (short-lived pores) are related to permeabilization (long-lived "transport" pores) only indirectly and confirm that we have to distinguish between the two types of pores.

The relationship and differences between transient pores and long-lived pores can be explained with the fast relaxation of the transient conductivity changes. When a cell is exposed to the high-voltage pulses the pore formation leads to an increase in the membrane conductivity and therefore the induced transmembrane voltage is decreased below U_c in the part of the cell membrane where $U_m > U_c$ [33–35,38]. However, since the transient changes of conductivity during the pulses relax in milliseconds after the pulses [21–23,26], U_m at the start of the next pulse (for 1 Hz repetition frequency 1 s later) again increases to the same value as at the start of the first pulse, consequently leading again to similar transient increase in conductivity and consequently to similar fraction of transient pores.

On the other hand, approximately linear increase in fraction of long-lived "transport" pores for increasing number of pulses shows that each consecutive pulse contributes to formation of new stable-pores. This suggests that there is approximately the same probability of formation of a stable pore during each pulse, which can be explained with the fact that the induced transmembrane voltage U_m is during each pulse approximately the same due to the fast resealing of the short-lived pores. The process of formation of stable pores could be either stabilization of already present transient pores or an independent process.

Our results are in agreement also with observations of other authors [8,9,12,29,21–23,44] that transport pores have different nature from the transient pores. Several mechanisms for pore stabilization were suggested such as pore coalescence [19], involvement of membrane structures [45,46], anisotropic inclusions [47], stabilization of large pores due to the contribution in free energy of large conductive pores [48] and dynamic mismatches between lipid domains [49].

By analyzing the conductivity changes after the pulses with the model (see Appendix), which describes diffusion of ions through the permeable cell membrane we obtained the efflux coefficients k_N which are proportional with the fraction of the "transport" pores. In Fig. 7 we demonstrate that we can describe field dependent efflux coefficients in the range of used voltages with a simple model where $k_N = C_N\,(1-E_c/E)E^2$, incorporation the increases in permeability due to larger area of the cell membrane exposed to $|U| > U_c$ and due to higher energy which is available for the formation of pores. In contrast to some other studies exponential increase in permeability as $k \propto exp(E)$ [28] or $k \propto exp(E^2)$ [29] was not observed, however, the model as presented (Eq. (9)) is only phenomenological, since the true electric field in the membrane, when the pores start to form, is a complex function of time, voltage, radius of pores and the number of pores [19,50]. The pores in the membrane decrease the induced transmembrane voltage and consequently the electric field inside the membrane is decreased, which could explain a slower increase with E. The relation between the observed and analyzed parameters can be schematically represented as:

(i) transient conductivity changes during the N-th pulse:

$$\Delta\sigma^N_{tran} \rightarrow \sigma_m \rightarrow f_p = \frac{\sigma_m(1-E_c/E)}{\rho(E)\sigma_{0por}}, \tag{10}$$

(ii) efflux of ions after N pulses:

$$\Delta\sigma(N) \rightarrow k_N \rightarrow f_{per} \propto N \times (1-E_c/E)E^2, \tag{11}$$

where function $\rho(E)$ incorporates a complex time dependence of U_m on E and other parameters, details are given in our previous study [26].

We further used the efflux coefficients calculated from $N\times100$ μs+8×1 ms experiments for the prediction of time-dependent increase in conductivity for 8×100 μs pulsing protocol using our theoretical model (Eq. (9) and Eq. (A.8)) as presented in Fig. 8b. The time-dependent concentration of ions or molecules is obtained by numerical integration of the Eq. (A.7) which describes diffusion through the permeabilized membrane for given k_N. We obtained good agreement between theoretical model of diffusion and experimental values (Fig. 8), therefore this model can be applied also to predict diffusion of

molecules during electroporation. However, since diffusion of ions is faster than diffusion of molecules, the resealing can be neglected in case of ions but for molecules has to be incorporated in the model. Here we do not deal with the electrophoretic transport of charged molecules since this can be neglected in the case of small molecules and ions where pulses are short compared to diffusion constant and the diffusion is a dominant process. For the transport of a DNA molecule additional mechanisms are present [5,6,51,52] and thus a more complex analysis is needed.

In conclusion, several studies of electroporation showed a complex dependence of the transport on pulse parameters where no simple relationship could be obtained [10,13–15]. On the other hand several theoretical studies which considered formation of transient structures in the presence of the electric field do not analyze the properties of long-lived pores [17–20]. For this reasons we use analysis of ion diffusion after the pulses to directly observe and analyze directly "transport" pores and their dependence on the number of pulses and electric field strength.

In this study we present a simple theoretical model which describes the fraction of long-lived "transport" pores and efflux coefficient as an explicit function of the electric field and number of pulses, where efflux coefficient is defined as $k_N = C_N (1 - E_c/E)E^2$. The model can accurately describe the field dependence for the used range of electric fields as well as describes time dependent diffusion of ions, which can be used also to describe diffusion of molecules by incorporating the resealing dynamics. The important new results of this study is that by quantifying diffusion through the long-lived "transport" pores we obtained that the fraction of the "transport" pores f_{per} increases with higher electric field due to larger area of the cell membrane exposed to above critical voltage and due to more energy which is available for the formation of pores. Therefore formation of the long-lived pores is governed also by the electrostatic energy of the pores. However, since the total amount of uptake (number of molecules) is an integral over a time period which depends on the time constant of resealing, it is clear that this simple dependence on the electric field strength or energy is lost, when the transport of molecules is considered.

Another important results is that almost linear dependence of the efflux coefficient and fraction of transport pores on the number of pulses suggests that each pulse increases the probability for the formation (stabilization) of the transport pores. We show that each new pulse leads to an increased number of long-lived stable pores, which enable diffusion of ions and molecules, in contrast to short-lived pores, which due to fast relaxation do not contribute to diffusion.

Appendix A

In this section we analyze theoretically the changes of conductivity on the time scale of seconds, where diffusion of ions dominates. In our model we include the increase of cell volume fraction after pulse application due to the colloid-osmotic swelling of cells. By far the largest concentration difference between internal and external concentration in this pulsing medium is for K^+ ions ($c_e \approx 0$ mM, $c_i = 142$ mM) so only this ions will be considered in the following analysis and their contribution to the external conductivity. The diffusion of ions through the membrane is governed by Nernst–Planck equation

$$\frac{dn_e(x,t)}{dt} = -DS\frac{dc(x,t)}{dx} - \frac{zF}{RT}DSc(x,t)\frac{d\Psi(x,t)}{dx} \quad (A.1)$$

where n_e is the number of moles in the external medium, D is the diffusion constant ($\sim 2\times10^{-5}$ cm^2/s), c the molar concentration, S the total transport surface $S = N_c S_{por}$ of N_c permeabilized cells and Ψ the electric potential. In general D and S depend on time, pulse duration, electric field strength and number of pulses. The effective diffusion constant D' inside the pore is reduced due to the interactions of the ion with the pore walls, where D' is a complex function of the electric field inside the pore [21,28,54]. But since we analyze diffusion between or after pulses when $U_m \cong 0$ we can use the approximation [54,28] that D' is constant: $D' = D\ \exp(-0.43\ w_0)$, where w_0 is the is the energy of an ion inside center of a pore normalized to kT.

The diffusion of ions is a slow process compared to the duration of the electric pulses thus we can assume that the major contribution to efflux of ions occurs without the presence of the electric field and $\Delta\Psi$ is small. Therefore the second term in Eq. (A.1) can be neglected which leads to diffusion equation. By replacing the concentration gradient with $(c_e - c_i)/d$ and by taking into account that the sum of ions inside and outside remains constant, the equation further simplifies:

$$\frac{dc_e(t)}{dt} = -\frac{D'S(E,N)}{dVF(1-F)}\left(c_e(t) - Fc_i^0\right), \quad (A.2)$$

where c_i^0 is the initial internal concentration of K^+ ions, V represent total volume and function $S(E, N)$ describes the field dependent surface of all pores. If we further neglect the volume fraction changes and assume that S is approximately constant (resealing is slow compared to ion efflux), we obtain that the solution of the above equation is an exponential increase to maximum $c_e^{max} = F\ c_i^0$

$$c_e(t) = c_e^{max}\left[1 - \exp\left(-\frac{t}{\tau}\right)\right], \quad (A.3)$$

with a time constant τ and efflux coefficient k being dependent on the fraction of transport pores f_{per}:

$$\tau = \frac{1}{f_{per}}\frac{dR(1-F)}{3D'} \quad k = 1/\tau. \quad (A.4)$$

by measuring current and voltage during the train of successive pulses we obtain the change of the initial level of the conductivity, i.e. conductivity increase due to the ion efflux. Therefore we can express the measured change of conductivity with the change in the external concentration of ions: $\Delta\sigma(t) = u_{K+}Z_{K+}F_a c_e(t)$, where $Z_{K+} = 1$, u_{K+} is mobility of K^+ ions and F_a Faraday constant. Thus we obtain the relative change in the conductivity due to the ion efflux

$$\frac{\Delta\sigma_e(t)}{\sigma_0} = A[1 - \exp(-kt)],\ A = \frac{u_{K^+}F_a c_e^{max}}{\sigma_0}. \quad (A.5)$$

The change in the measured effective conductivity of a cell suspension can be obtained from Maxwell equation Eq. (5), where $\sigma_p = 0$:

$$\Delta\sigma = \Delta\sigma_e \frac{(1+F)}{(1-0.5F)}. \quad (A.6)$$

Now we have to consider a general case where the efflux coefficient depends on the number of pulses which were used; $k_N = k$ (N-th pulse). Now the time dependent $\Delta\sigma$ is a sum of the terms between the pulses:

$$\frac{\Delta\sigma(t)}{\sigma_0} = \sum_N A_N[1 - \exp(-k_N t)]. \quad (A.7)$$

Form this it follows that the efflux coefficient after the N-th pulse can be determined from the measured conductivity at N-th pulse ($\Delta\sigma_N$) and at $N+1$-th pulse ($\Delta\sigma_{N+1}$):

$$k_N = \frac{1}{\Delta t_N} \ln\left[1 - \frac{\Delta\sigma_N}{\Delta\sigma_{max}} / 1 - \frac{\Delta\sigma_{N+1}}{\Delta\sigma_{max}}\right], \quad (A.8)$$

where Δt_N is the time difference between N-th and $N+1$-th pulse, and $\Delta\sigma_{max}$ is the maximum value of the conductivity, i.e. the saturation point when the concentrations inside and outside the cell are equal. From the efflux coefficient k_N the fraction of pores can be estimated using Eq. (A.4):

$$f_{per}^N \approx k_N \frac{dR(1-F)}{3D'}. \quad (A.9)$$

Appendix B. Supplementary data

Supplementary data associated with this article can be found, in the online version, at doi:10.1016/j.bbagen.2006.06.014.

Acknowledgements

This research was supported by the Ministry of High Education, Science and Technology of the Republic of Slovenia under the grants Z2-6503-1538 and P2-0249. Authors thank also Peter Kramar and Matej Reberšek (both Faculty of Electrical Engineering, University of Ljubljana) for their contribution at development of Cliniporator device which was developed within the 5th framework under the grant Cliniporator QLK3-99-00484 funded by the European Commission.

References

[1] M. Okino, H. Mohri, Effects of a high-voltage electrical impulse and an anticancer drug on in vivo growing tumors, Jpn. J. Cancer Res. 78 (1987) 1319–1321.
[2] L.M. Mir, Therapeutic perspectives of in vivo cell electropermeabilization, Bioelectrochemistry 53 (2000) 1–10.
[3] G. Serša, S. Kranjc, M. Čemaar, Improvement of combined modality therapy with cisplatin and radiation using electroporation of tumors, Int. J. Radiat. Oncol., Biol. Phys. 46 (2000) 1037–1041.
[4] E. Neumann, M. Schaefer-Ridder, Y. Wang, P.H. Hofschneider, Gene transfer into mouse lyoma cells by electroporation in high electric fields, EMBO J. 1 (1982) 841–845.
[5] S.I. Sukharev, V.A. Klenchin, S.M. Serov, L.V. Chernomordik, Y.A. Chizmadzhev, Electroporation and electrophoretic DNA transfer into cells. The effect of DNA interaction with electropores, Biophys. J. 63 (1992) 1320–1327.
[6] M.J. Jaroszeski, R. Heller, R. Gilbert, Electrochemotherapy, Electrogenetherapy and Transdermal Drug Delivery: Electrically Mediated Delivery of Molecules to Cells, Humana Press, New Jersey, 1999.
[7] N. Pavšelj, V. Préat, DNA electrotransfer into the skin using a combination of one high- and one low-voltage pulse, J. Controlled Release 106 (2005) 407–415.
[8] U. Zimmermann, Electric field-mediated fusion and related electrical phenomena, Biochim. Biophys. Acta 694 (1982) 227–277.
[9] E. Neumann, A.E. Sowers, C.A. Jordan, Electroporation and Electrofusion in Cell Biology, Plenum Press, New York, 1989.
[10] M.P. Rols, J. Teissie, Electropermeabilization of mammalian cells: quantitative analysis of the phenomenon, Biophys. J. 58 (1990) 1089–1098.
[11] T.Y. Tsong, Electroporation of cell membranes, Biophys. J. 60 (1991) 297–306.
[12] J.C. Weaver, Y.A. Chizmadzhev, Theory of electroporation: a review, Bioelectrochem. Bioenerg. 41 (1996) 135–160.
[13] M.P. Rols, J. Teissie, Ionic-strength modulation of electrically induced permeabilization and associates fusion of mammalian cells, Eur. J. Biochem. 179 (1989) 109–115.
[14] P.J. Canatella, J.F. Karr, J.A. Petros, M.R. Prausnitz, Quantitative study of electroporation-mediated molecular uptake and cell viability, Biophys. J. 80 (2001) 755–764.
[15] T. Kotnik, A. Maček-Lebar, D. Miklavčič, L.M. Mir, Evaluation of cell membrane electropermeabilization by means of a nonpermeant cytotoxic agent, BioTechniques 28 (2000) 921–926.
[16] A. Maček-Lebar, D. Miklavčič, Cell electropermeabilization to small molecules in vitro: control by pulse parameters, Radiol. Oncol. 35 (2001) 193–202.
[17] L.V. Chernomordik, S.I. Sukarev, S.V. Popov, V.F. Pastushenko, A.V. Sokirko, I.G. Abidor, Y.A. Chizmadzev, The electrical breakdown of cell and lipid membranes: the similarity of phenomenologies, Biochim. Biophys. Acta 902 (1987) 360–373.
[18] I.P. Sugar, E. Neumann, Stochastic model for electric field-induced membrane pores electroporation, Biophys. Chem. 19 (1984) 211–225.
[19] R.W. Glaser, S.L. Leikin, L.V. Chernomordik, V.F. Pastushenko, A.V. Sokirko, Reversible electrical breakdown of lipid bilayers: formation and evolution of pores, Biochim. Biophys. Acta 940 (1988) 275–287.
[20] H. Leontiadou, A.E. Mark, S.J. Marrink, Molecular dynamics simulations of hydrophilic pores in lipid bilayers, Biophys. J. 86 (2004) 2156–2164.
[21] K. Kinosita, T.Y. Tsong, Voltage-induced pore formation and hemolysis of human erythrocytes, Biochim. Biophys. Acta 471 (1977) 227–242.
[22] K. Kinosita, T.Y. Tsong, Formation and resealing of pores of controlled sizes in human erythrocyte membrane, Nature 268 (1977) 438–441.
[23] K. Kinosita, T.Y. Tsong, Voltage-induced conductance in human erythrocyte, Biochim. Biophys. Acta 554 (1979) 479–497.
[24] I.G. Abidor, A.I. Barbul, D.V. Zhelev, P. Doinov, I.N. Bandarina, E.M. Osipova, S.I. Sukharev, Electrical properties of cell pellets and cell fusion in a centrifuge, Biochim. Biophys. Acta 1152 (1993) 207–218.
[25] I.G. Abidor, L.-H. Li, S.W. Hui, Studies of cell pellets: II. Osmotic properties, electroporation, and related phenomena: membrane interactions, Biophys. J. 67 (1994) 427–435.
[26] M. Pavlin, M. Kandušer, M. Reberšek, G. Pucihar, F.X. Hart, R. Magjarević, D. Miklavčič, Effect of cell electroporation on the conductivity of a cell suspension, Biophys. J. 88 (2005) 4378–4390.
[27] R. Shirakashi, C.M. Kostner, K.J. Muller, M. Kurschner, U. Zimmermann, V.L. Sukhorukov, Intracellular delivery of trehalose into mammalian cells by electropermeabilization, 189 (2002) 45–54.
[28] K. Schwister, B. Deuticke, Formation and properties of aqueous leaks induced in human erythrocytes by electrical breakdown, Biochim. Biophys. Acta 816 (1985) 332–348.

[29] M. Schmeer, T. Seipp, U. Pliquett, S. Kakorin, E. Neumann, Mechanism for the conductivity changes caused by membrane electroporation of CHO cell-pellets, Phys. Chem. Chem. Phys. 6 (2004) 5564–5574.
[30] G. Pucihar, L.M. Mir, D. Miklavčič, The effect of pulse repetition frequency on the uptake into electropermeabilized cells in vitro with possible applications in electrochemotherapy, Bioelectrochemistry 57 (2002) 167–172.
[31] M. Pavlin, N. Pavšelj, D. Miklavčič, Dependence of induced transmembrane potential on cell density, arrangement and cell position inside a cell system, IEEE Trans. Biomed. Eng. 49 (2002) 605–612.
[32] K.A. DeBruin, W. Krassowska, Modeling electroporation in a single cell. I. Effects of field strength and rest potential, Biophys. J. 77 (1999) 1213–1223.
[33] M. Hibino, H. Itoh, K. Kinosita Jr., Time courses of cell electroporation as revealed by submicrosecond imaging of transmembrane potential, Biophys. J. 64 (1993) 1789–1800.
[34] M. Hibino, M. Shigemori, H. Itoh, K. Nagayama, K. Kinosita Jr., Membrane conductance of an electroporated cell analyzed by submicrosecond imaging of transmembrane potential, Biophys. J. 59 (1991) 209–220.
[35] B. Gabriel, J. Teissie, Time courses of mammalian cell electropermeabilization observed by millisecond imaging of membrane property changes during the pulse, Biophys. J. 76 (1999) 2158–2165.
[36] M. Pavlin, D. Miklavčič, Effective conductivity of a suspension of permeabilized cells: a theoretical analysis, Biophys. J. 85 (2003) 719–729.
[37] M. Pavlin, T. Slivnik, D. Miklavčič, Effective conductivity of cell suspensions, IEEE Trans. Biomed. Eng. 49 (2002) 77–80.
[38] S. Takashima, Electrical Properties of Biopolimers and Membranes, Adam Hilger, Bristol, 1989.
[39] V.B. Bregar, Effective-medium approach to the magnetic susceptibility of composites with ferromagnetic inclusions, Phys. Rew. B 71 (2005) 174418 (8).
[40] V.B. Bregar, M. Pavlin, Effective-susceptibility tensor for a composite with ferromagnetic inclusions: enhancement of effective-media theory and alternative ferromagnetic approach, J. Appl. Phys. 95 (2004) 6289–6293.
[41] J.C. Maxwell, Treatise on Electricity and Magnetism, Oxford University Press, London, 1873.
[42] R.V. Davalos, B. Rubinsky, D.M. Otten, A feasibility study for electrical impedance tomography as a means to monitor tissue electroporation for molecular medicine, Biomed. Eng. IEEE Tran. Biomed. Eng. 49 (2002) 400–403.
[43] A.S. Khan, M.A. Pope, R. Draghia-Akli, Highly efficient constant-current electroporation increases in vivo plasmid expression, DNA Cell Biol. 24 (2005) 810–818.
[44] J. Teissie, C. Ramos, Correlation between electric field pulse induced long-lived permeabilization and fusogenicity in cell membranes, Biophys. J. 74 (1998) 1889–1898.
[45] M.P. Rols, J. Teissie, Experimental evidence for the involvement of the cytoskeleton in mammalian cell electropermeabilization, Biophys. J. 1111 (1992) 45–50.
[46] J. Teissie, M.P. Rols, Manipulation of cell cytoskeleton affects the lifetime of cell-membrane electropermeabilization, Ann. N. Y. Acad. Sci. 720 (1994) 98–110.
[47] M. Fošnarič, V. Kralj-Iglič, K. Bohinc, A. Iglič, S. May, Stabilization of pores in lipid bilayers by anisotropic inclusions, J. Phys. Chem. B 107 (2003) 12519–12526.
[48] K.C. Smith, J.C. Neu, W. Krassowska, Model of creation and evolution of stable electropores for DNA delivery, Biophys. J. 86 (2004) 2813–2826.
[49] J. Teissie, M. Golzio, M.P. Rols, A minireview of our present (lack of ?) knowledge, Biochim. Biophys. Acta 1724 (2005) 270–280.
[50] A. Parsegian, Energy of an ion crossing a low dielectric membrane: solutions to four relevant electrostatic problems, Nature 221 (1969) 844–846.
[51] S. Šatkauskas, F. Andre, M.F. Bureau, D. Scherman, D. Miklavčič, L.M. Mir, Electrophoretic component of electric pulses determines the efficacy of in vivo DNA electrotransfer, Hum. Gene Ther. 16 (2005) 1194–1201.
[52] E. Phez, C. Faurie, M. Golzio, J. Teissie, M.P. Rols, New insights in the visualization of membrane permeabilization and DNA/membrane interaction of cells submitted to electric pulses, Biochim. Biophys. Acta 1724 (2005) 248–254.